VNU Journal of Science: Earth and Environmental Sciences, Vol. 31, No. 3 (2015) 1-14

Permanent Water Bodies Mapping in the Mekong River Delta Using Seasonal Time Series C-band SAR Data

Nguyễn Bá Duy*, Trần Thị Hương Giang

Hanoi University of Mining and Geology, Vietnam

Received 13 August 2014

Revised 10 September 2014; Accepted 6 August 2015

Abstract: Microwave remote sensing or SAR (Synthetic Aperture Radar) data has been employed extensively to map open water bodies and to monitor flood extents, where cloud cover often prohibits the use of satellite sensors operating at other wavelengths. Where total inundation occurs, a low backscatter return is expected due to the specular reflection of SAR signal on the water surface. However, low local incidence angle and wind induced waves can cause a roughening of the water surface which result in a high return signal. It is also mean that the temporal variability (TV) of the backscatter from water bodies is higher than other land surfaces. The Mekong River Delta is a region with very long wet season (starting in May and lasting until October-November), resulting in almost crop fields also has low backscatter returns. Where such conditions occur adjacent to open water, this can make the separation of water and land problematic using SAR data. In this paper, we use seasonal time series C-band SAR data (dry season), we also examine how the variability in radar backscatter with incidence angle may be used to differentiate water from land overcoming. We carry out regression over multiple sets of seasonal time series data, determined by a moving window encompassing consecutively-acquired ENVISAT ASAR Wide Swath Mode data, to derive three backscatter model parameters: the slope β of a linear model fitting backscatter against local incidence angle; the backscatter normalized at 50° using the linear model coefficients $\sigma^{o}(50^{o})$, and the minimum backscatter (MiB) from time series data after normalized. A comparison of the three parameters (β, TV and MiB) shows that MiB in combination with TV provides the most robust means to segregate water from land by a simple thresholding algorithm.

Keywords: Water bodies mapping, SAR, time series analysis.

1. Introduction

The mapping of permanent water plays an importaint role across several fields. In recent years, much attention has benn paid to monitoring of wesland ecosystems, in which inundation patterns are formative in the study of biodiversity and greenhouse gas emissions [1-3].

* Corresponding author. Tel.: 84-904485651.
Email: nguyenbaduy@humg.edu.vn

Radar has several advantages over visual-infra red (VIR) data - being an active sensor system, it can acquire data independently from the position of the sun. Perhaps most importantly, radar can penetrate the cloud cover that prohibits, to varying degrees, the use of VIR data for continuous flood monitoring, or for timely production of flood maps for disaster response purposes. To take full advantage of radar data, much research has been concerned with the task of overcoming some difficulties in the interpretation of radar images. Spaceborne Synthetic Aperture Radar (SAR) data are available from number of satellites operating at different wavelengths, with multi-mode image different acquisition strategies. Typically, the configuration and are operated with acquisition of high resolution SAR systems (1- 20m) targets specific areas. Sensors with acquisition modes at moderate resolution (100-1000m) are instead operated to acquire data on a global scale in a repeated manner. In view of generating estimates of a land surface parameter for large areas, moderate resolution image data products become the only practical alternative if a mapping of repeated acquisitions is of advantage since multi-temporal observations allow reduction of speckle noise [4], detection of trends in land surface parameters such as soil moisture [5], wetlands [3, 6], and cropland and water bodies.

Flat, open water acts as a specular reflector of radar energy away from the sensor. For this reason, water under certain conditions is characterised by a low backscatter return. However, where structures such as vegetation, steep land forms and man-made features emerge through the surface of the water, multiple interactions between such structures and the surface of the water cause “double bounce” effects, which result in a very high return signal. Depending on the relative scale and density of these features with the pixel size of the data image, the result is either a mixed pixel mid-value aggregate of low and high backscatter returns,being hard to distinguish from dry land, or a very high backscatter value, which in turn can be very hard to distinguish from wet soil or vegetation. Consequently, the major limitation of single SAR backscatter images to map water bodies relies in the dependence of backscattered signal upon surface conditions of water body. Thresholding approaches or supervised approaches applied to a single image were sufficient to detect and delineate lakes and rivers in C and X-band co-polarized data as long as the backscatter was overall low with respect to other land surfaces. Several authors reported false detections of water as land in the case of rugged water surface [7, 8]. A combination of classifications based on SAR amplitude and interferometry SAR coherence using individual threshold-based approaches on each observable. Classification accuracy reported in terms of correctness and completeness was between 51% and 72%, and 60% and 81%, respectively [9] Slightly higher accuracy was obtained when using coherence data only [9].

Multi-temporal observations were used to understand and quantify dynamics of water bodies [1, 6, 10]; a general conclusion was that the temporal sampling even in the case of very frequent observations as in the case ENVISAT ASAR ScanSAR images was not optimal to track dynamics in a sufficiently detailed manner. Moreover, the affecting of difference local incidence angle for each pixel location in image is still available that potentially lowers the accuracy of classification results. Two main approaches for local normalization of time series SAR data are cosine normalization approaches based on the Lambert’s of optics and empirical, regression based approaches. However, no previous studies in rice mapping apply these local incidence normalization approaches. In this study, we performed local incidence angle normalization by using empirical, regression based approaches to the data to minimize impacts on the mapping results prior to analysis.

The objective of this paper is to investigate the properties of metrics (slope, temporal variability and minimum backscatter) derived from multi-temporal SAR data and demonstrate their usefulness in the detection of permanent water bodies.

The SAR dataset consisted of images of the radar backscattered intensity acquired by ENVISAT Advanced SAR (ASAR) instrument. To assess the consistency of multi-temporal metrics and the robustness of the water body mapping approach from SAR data here considered, investigations were undertaken at Mekong River Delta.

2. Study area and dataset

2.1. Study area description

The study area is Mekong Delta, the major rice-producing area in Vietnam,it produces more than half of the rice in Vietnam.

The Mekong Delta is a region constituted by 13 provinces in the southern of the country, covering around 40000 km. The topography is very flat with most land below 5m(see Figure 1) The climate is tropical (8.5N - 11N in latitude), with the wet season starting in May and lasting until October-November, and the dry season from December to April. Rice cultivation is the major agricultural activity in this area (approximately 2 million hectares of paddy), rice producing yield of this area contributes about 51% of the total yield of the country) and it is largely supported by various agro-hydrological factors such as rainfall and irrigation (Results of the 2011 Rural, Agricultural and Fishery Census, General Statistics Office of Vietnam).

2.2. Dataset

2.2.1. ENVISAT WSM data

This paper uses data acquired by the Wide Swath mode of the ASAR on board of the European Environmental Satellite ENVISAT. ENVISAT was launched on March 1, 2002, and it circles the Earth in a sun-synchronous orbit at an altitude of approximately 800 km with a nominal repeat rate of 35 days, covers a swath of 405 km, with a spatial resolution of 150 m and incidence angle in each image ranges from 17^0 to 42^0. A total of 132 ASAR WS images which are completely or partially covering over the Mekong River delta, between March 2007 and March 2011, the following ENVISAT WS data (Fig 2) was acquired from European Space Agency (ESA). In order to monitor rice agricultural by means of methods based on the temporal backscatter behavior characterization. Images were acquired with HH polarization and during both descending (morning) and ascending (evening) overpasses. Based on characterization of the backscattered of water that illustrated (see Figure 3); for this study, five year dry season dataset (22 images) of all ENVISAT ASAR WSM images over the study area was considered. It was assumed that the number of backscatter observations collected seasonally would have been sufficient.

2.2.2. Optical data

LANDSAT 7 ETM^+ and LANDSAT 5 images (path/row: 125/053, 125/054 and 126/053) is acquired through the USGS website http://earthexplorer.usgs.gov/ and were used as a reference parameter to generate training data which was later used to estimate threshold and validating the accuracy of classification results (Fig 4). Table 1 lists the available dates for all

LANDSAT over study area for a period of 5 years (2007-2011). The data have been geometrically and radiometrically corrected for spectral bands.

High-resolution imagery in global image and map viewers such as Google Earth in combining with Landsat time series data are an alternative approach to generate reference information. In this study, a stratified random sampling approach has been developed to select water samples in manner. Polygons corresponding to a pixel in the SAR image were overlaid onto Google Earth image.

2.2.3. Land use land cover data

Ancillary maps, including the land use land cover map of 13 provinces in the study at 1/50,000 (2010) collected from the General Department of Land Administration of Vietnam. Because the land use data just have been updated every a few years and are recorded in vector format, thus we used the land use land cover map in combine with Landsat time series data to digitize sampling sites of homogeneous permanent water body for water class that had not changes between 2007 and 2011. Digitizing sampling sites then were converted to a raster file (75 m resolution) which used for validation.

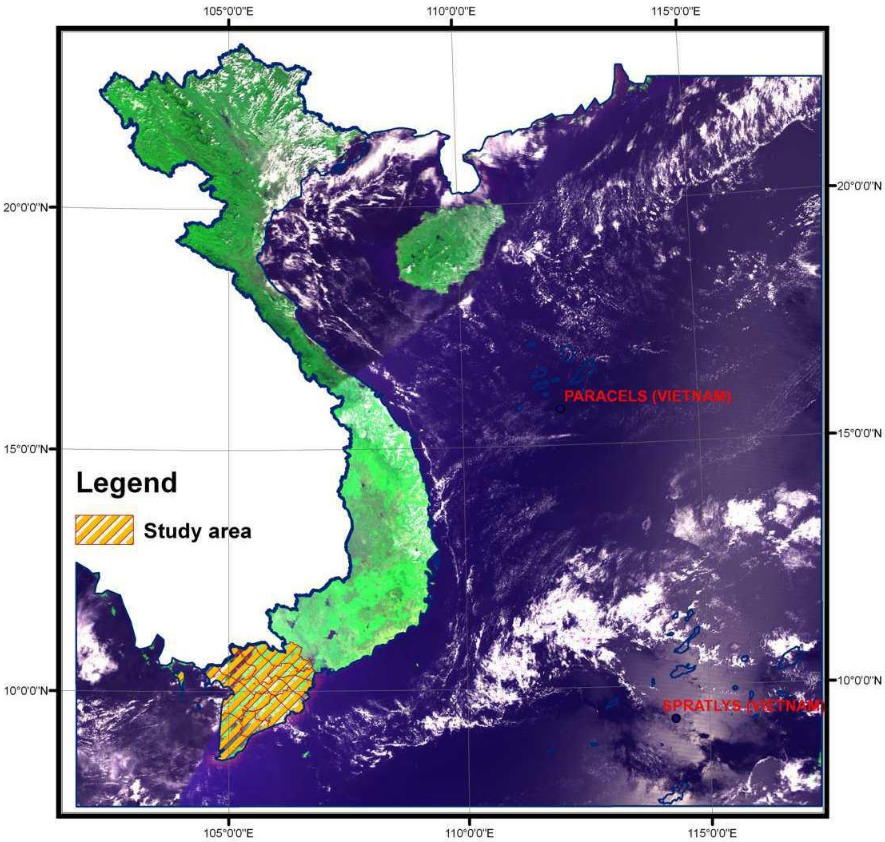

Fig. 1. Study area.

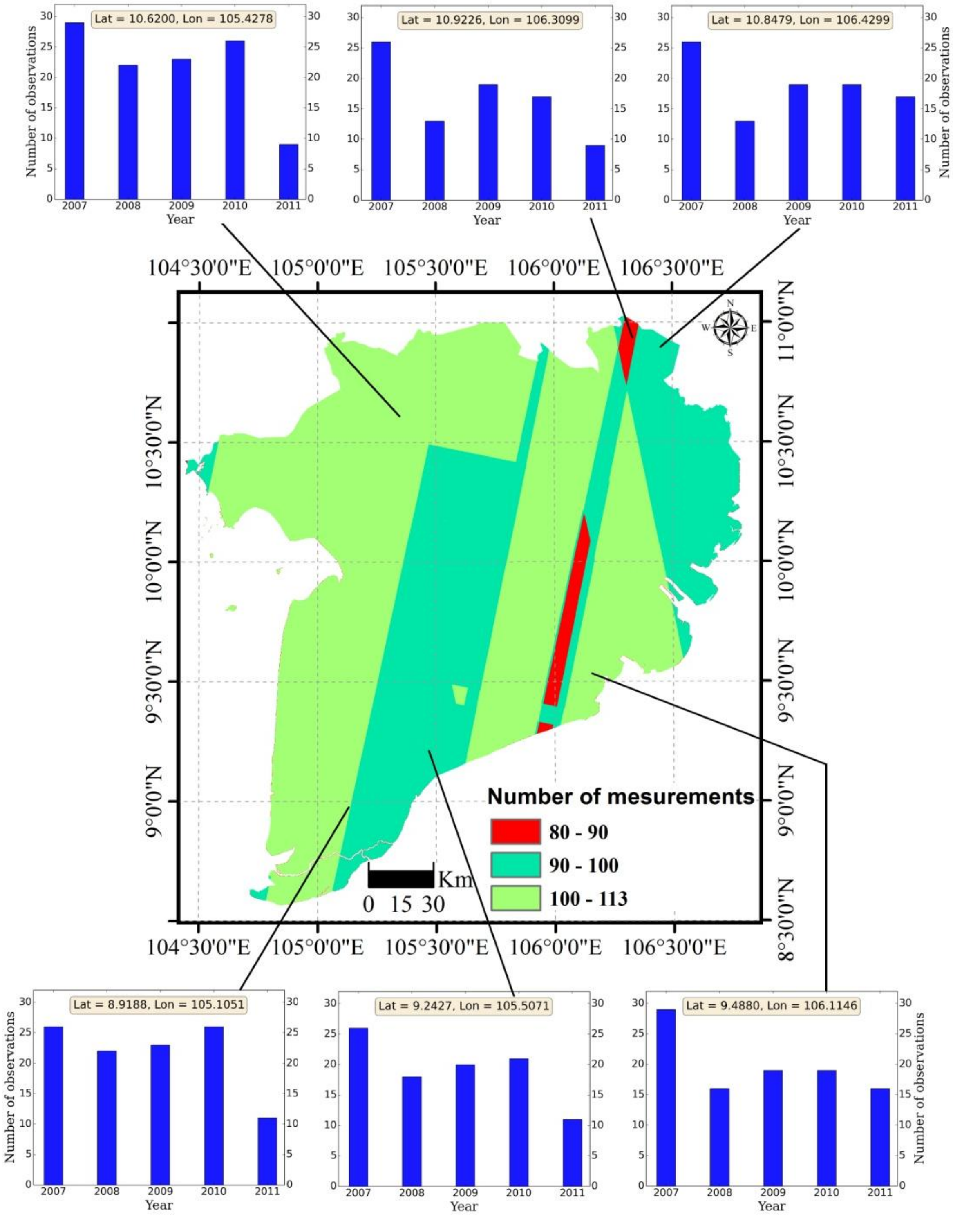

Fig. 2. The number of ASAR WSM images over study area for a period of 5 years (2007-2011).

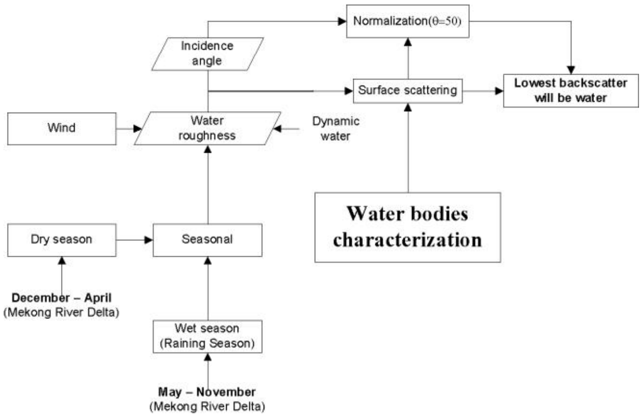

Fig. 3. Water body characterization.

Table 1. ENVISAT ASAR WSM data sets used for permanent water bodies mapping in the Mekong Delta (Scenes acquired during the dry season)

2007	2008	2009	2010	2011
2007-Mar-01	2008-Jan-10	2009-Dec-10	2010-Jan-14	2011-Jan-01
2007-Dec-06	2008-Feb-14	2009-Dec-13	2010-Jan-17	2011-Jan-14
2007-Dec-25	2008-Apr-08		2010-Feb-18	2011-Feb-02
	2008-Apr-15		2010-Dec-14	2011-Mar-04
	2008-Apr-24		2010-Dec-15	2011-Mar-15
	2008-Apr-27			2011-Apr-03

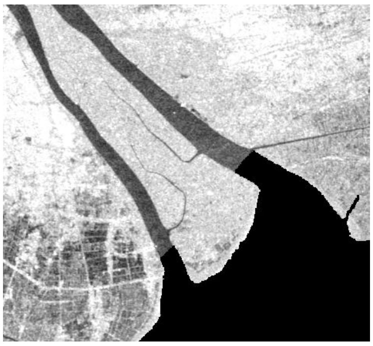

a) ENVISAT WSM 15-November-2010

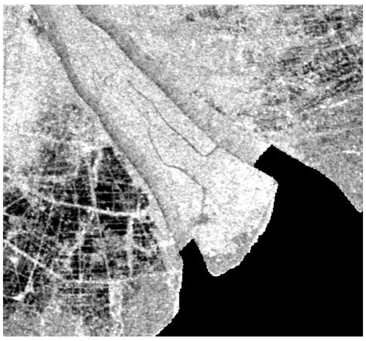

b) ENVISAT WSM 23-June-2011

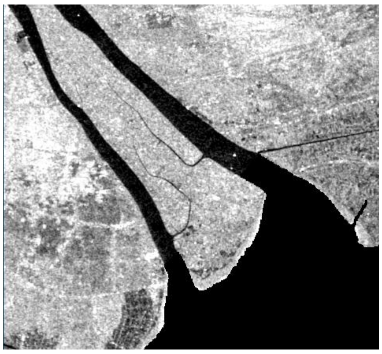

b) ENVISAT WSM 15-Mar-2011

d) LANDSAT-8 TCC (09-Dec-2009)

Fig. 4. *Influence of wind* and local incidence angle to radar backscatter.

3. Data pre-processing and signature analysis

In a single date ENVISAT ASAR image, water body areas are showed in black. Minimum radar echo is generally due to the fact that water bodies, with its smooth surface, act as specular reflectors of incoming radar signals, resulting in weak return towards to the sensor. But rough water surface (influenced by strong wind, current flows) may return radar signal of varying strength, visible by different grey levels due to "Bragg resonance" effect. In the case of multi-temporal images, the water body areas affected by strong wind are seen as various colors, especially in rainy season (Figure 4a). Otherwise, the main factor affecting SAR imaging of water body areas is incidence angle, at smaller incidence angles, the specular reflection from the standing water gives very high radar return in the image (Figure 4b). These two factors must therefore be considered when interpreting multi-temporal SAR images for permanent water body mapping. To overcome these two weakness; first, data selection has chosen as mention in section 2.2, second, backscatter need to be normalized at a low reference angle (it is presented in the next section and Fig 5).

3.1. Data pre-processing

For geocoding and radiometric calibration using NEST software developed by the *European Space Agency* (ESA). NEST produces the sigma nought image and, using a model of the satellite orbit and a Digital Elevation Model (DEM), the corresponding local incidence angle estimates. DORIS precise orbit data and 30 arc-seconds DEM (SRTM) were used. The resampling of these images to a fixed grid (cover all the study area) in a database was carried out in order to allow efficient time series analysis, which was required for the extraction of the backscatter parameters.

A linear model was fitted to the time series of sigma nought (σ^o) and local incidence angle (θ) measurements at each grid point, according to Eq. (2), resulting in the backscatter model parameters slope (k) and intercept (m). Such linear models have been applied in other studies, e.g. in the case of RADARSAT data [11] and ERS Scatterometer data [12].

$$\sigma^o(\theta) = m + k\theta \qquad (1)$$

The fitting of the linear model using the least-squares method was implemented based input time series SAR datasets.

3.2. Signature analysis

The parameters retrieved from time series SAR metrics considered in this study were the slope, maximum backscatter (MaB), minimum backscatter (MiB) and the temporal variability (TV) of the backscatter defined as the standard deviation of the backscatter intensities in the logarithmic decibel (dB) scale (for both after and before normalization). The use of the dB scale for the latter parameter enhanced the contrast with respect to a standard deviation based on intensities in the linear scale.

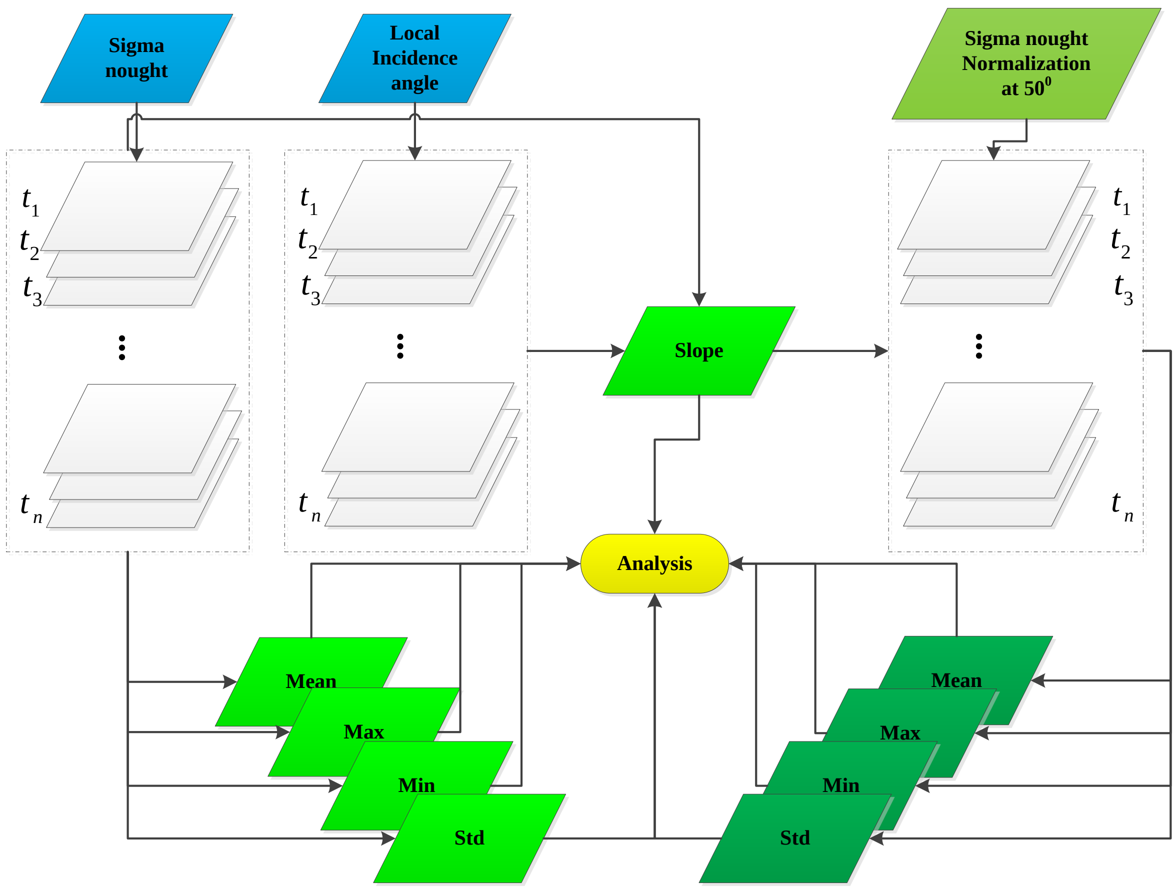

Fig. 5. Backscatter normalization and signature analysis.

a) Min backscatter before normalization

b) Min backscatter after normalization at 50^0

c) Standard deviation of the backscattered

Fig. 6. Parameters retrieval from time series ENVISAT WSM SAR data.

Based on visualization and analysis, two parameters have the most potential apply for permanent water body extraction has been chosen for data analysis. They are minimum backscatter after normalization at 50^0(MiB) and the temporal variability before normalization (TV). Fig. 6 shows the image of TV and MiB for the study area. Permanent water bodies in the east of the study area were characterized by highest TV and lowest MiB. To get understanding for the behavior of TV and MiB of water and land surfaces, Fig. 7 shows the time series of the SAR backscatter for three pixels labeled in land cover as water body, cropland and urban, respectively. As can be seen that the variation of the SAR backscatter in seasonal time over open water implied the lowest MiB among the three cases here considered because of the repeated occurrence of specular scattering in forward direction (ie., calm wind condition and high local incidence angle). The variation of open water and cropland before normalization quite similar and TV of cropland and permanent water body are almost equal, 4.45 dB and 4.72 dB respectively because of the characteristic of cultivate activity and very low terrain elevation (cropland almost has water in time). Otherwise TV of cropland was affected by changes of the backscatter during the growing season. The TV of urban was very low since the backscatter was rather constant in time.

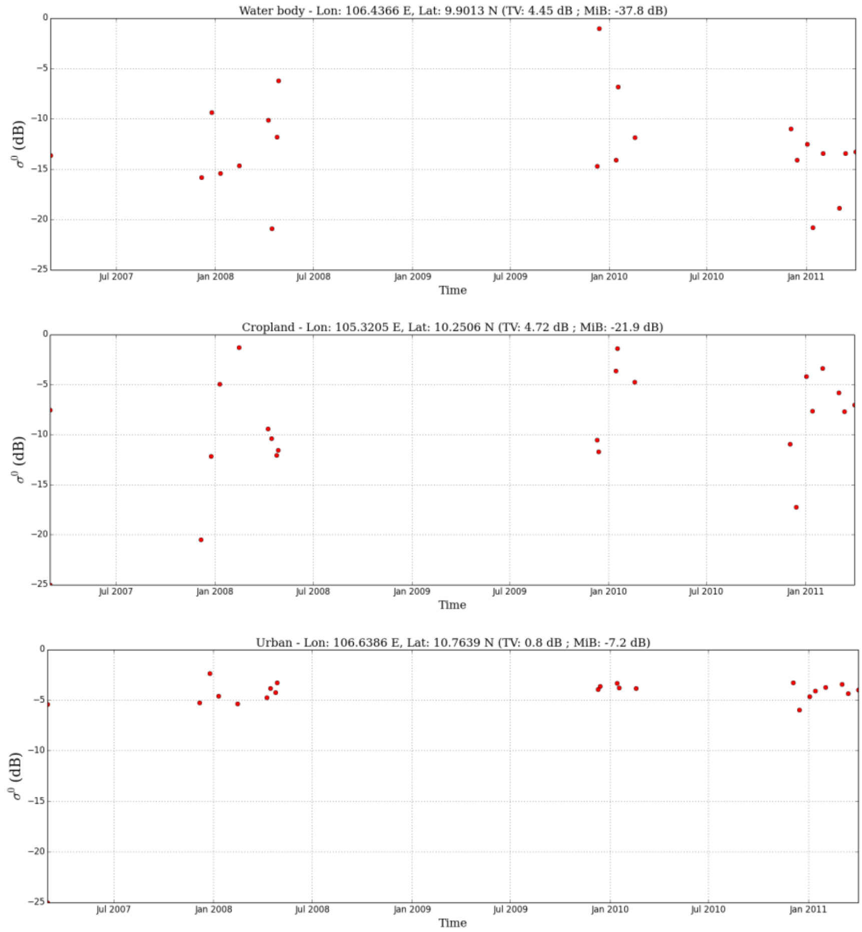

Fig. 7. Time series SAR backscatter for three pixels labeled in land cover as water body, cropland and urban, respectively. TV and MiB estimates are presented above corresponding panel.

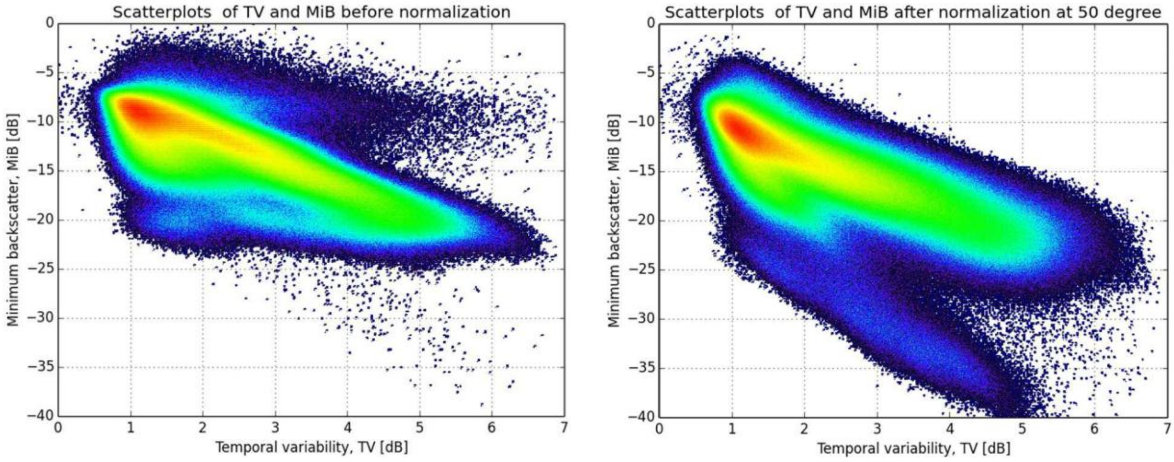

a) TV vs MiB (before normalization) *b) TV vs MiB (after normalization)*

Fig. 8. Density plot of TV and MiB for all pixels the entire study area.

The different behavior of TV and MiB over water and land is further shown by the density plots in Fig. 8 for the study area. The combination of TV and MiB (after normalization) better than the combination of Tv and MiB (before normalization): It showed a clear separation between the water and other land cover. Water present high TV and low MiB in consequence of the strong variability of the SAR backscatter in time and low return at high local incidence angle and under calm conditions resulting in specular reflection in the forward direction, respectively

4. Permanent Water body classification methodology

The scatterplots of TV and MiB for all pixels in the entire study area showed symmetry of TV and MiB (after normalization at 50^0) for water and non-water with respect to a diagonal line represented by linear equation of increasing TV for decreasing MiB. A simple thresholding rule in the feature space of TV and MiB seemed to be sufficient to extract permanent water areas from non-water areas. In this study, we defined the thresholding rule as the diagonal line that was at equal distance from pre-defined clusters of "pure" and "pure" land based on training dataset.

Equation (2) corresponds to the diagonal line representing the threshold in the feature space of TV and MiB:

$$Y = -2,71x - 17.5 \qquad (2)$$

Here, x represents the TV in dB and y represents the MiB in dB.This thresholding rule was found to yield a very good separation between pure land and pure water in the Mekong River Delta study area (Fig. 9). Ultimately, we preferred setting up a simple classification approach to understand the potential of the TV and MiB to separate water and non-water rather than proceeding with a more complex algorithm already available in current investigations.

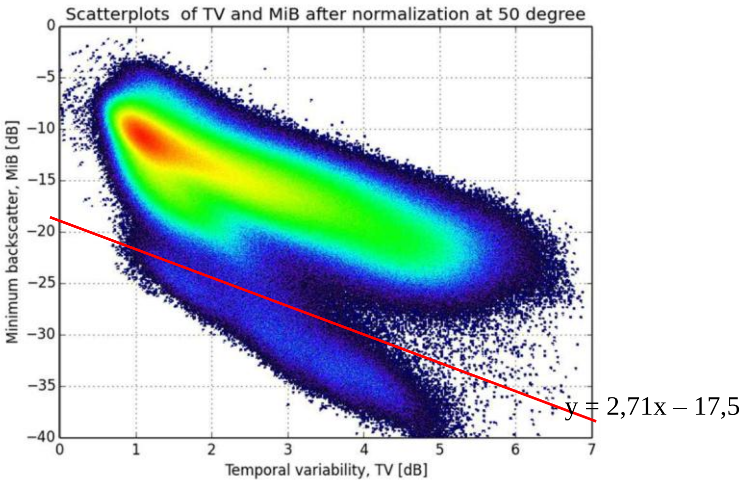

Fig. 9. Illustration of the water body mapping algorithm. Decision rules are represented by the Red diagonal line. The water and the non-water regions in the feature space of the TV and MiB are masked according to red line.

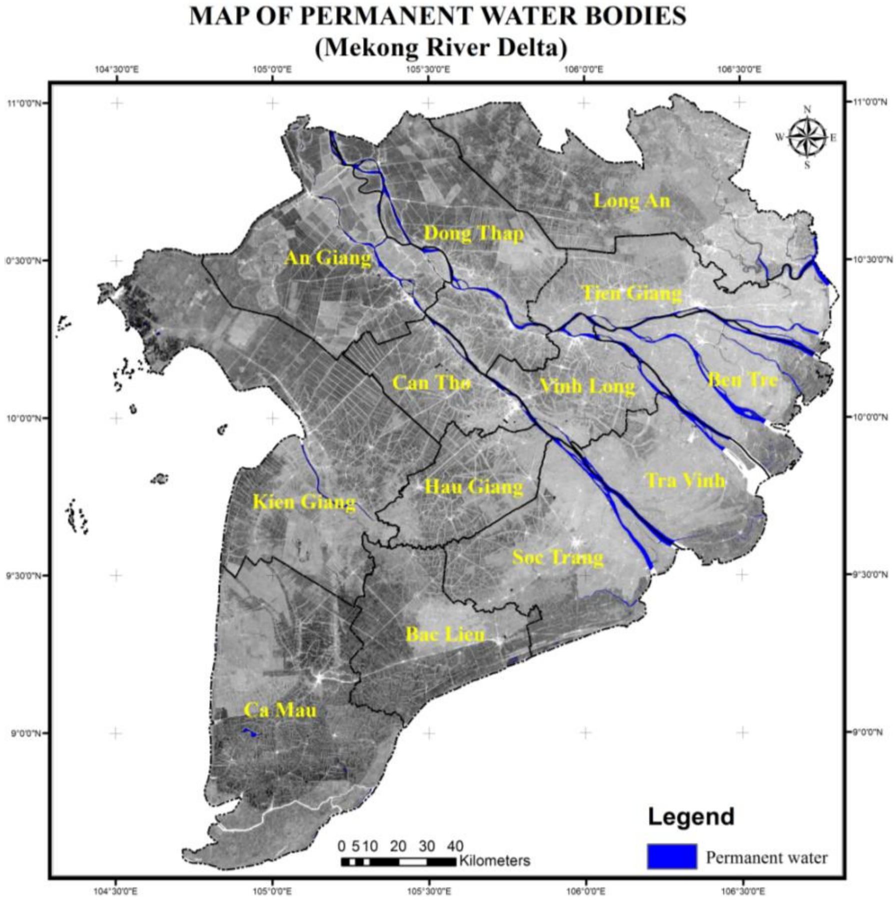

Fig. 10. Map of permanent water bodies in Mekong River Delta.

5. Assessment of permanent water body mapping accuracy

Verification of the permanent water body maps obtained from ENVISAT ASAR WSM data is provided in the form of percentages of agreement with respect to the samples extracted from ground reference data created after combining Landsat time series data and land use land cover map conducted in 2010. Regardless of the reference dataset, we use the terms of user's and producer's accuracy (UA and PA) as defined in to quantify the agreement between time series parameter retrieval from SAR-based classification and a reference dataset.

The goal of object detection is usually a distinction between two classes, object and background. Comparing the results of the automated extraction to reference data, an entity classified as an object that also corresponds to an object in the reference is classified as a True Positive (TP). A False Negative (FN) is an entity corresponding to an object in the reference that is classified as background, and a False Positive (FP) is an entity classified as an object that does not correspond to an object in the reference. A True Negative (TN) is an entity belonging to the background both in the classification and in the reference data [13]. The confusion matrix has a very simple structure. Two metrics for the quality of the result, the *Completeness* (Comp) is referred to as *Producer's Accuracy*, and the *Correctness* (Corr) also referred to as *User's Accuracy* [14].

$$Comp = \frac{\|TP\|}{\|TP\| + \|FN\|} \quad (3)$$

$$Corr = \frac{\|TP\|}{\|TP\| + \|FP\|} \quad (4)$$

A good classification should have both a high completeness and correctness. The *Quality* of the results provides a compound performance metric that balances completeness and correctness.

$$Quality = \frac{\|TP\|}{\|TP\| + \|FP\| + \|FN\|}$$

$$Quality = \frac{Comp * Corr}{Comp + Corr - Comp * Corr}$$

Table 2. Accuracy assessments of permanent water bodies class

	Comp	Corr	Quality
Water	97.3%	96.0%	93.7%

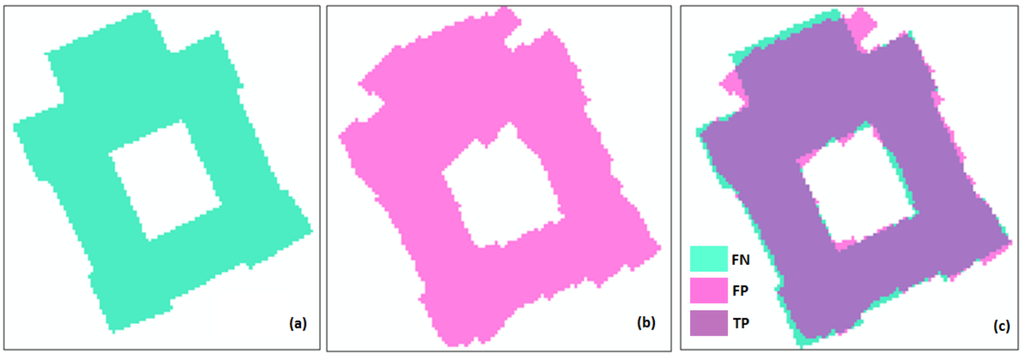

Fig. 11. (a) Ground truth data; (b) classified result; (c) Ground truth data overlay with classified result.

6. Conclusions

In this study, we looked at the potential of SAR multi-temporal metrics for permanent water body retrieval with particular regard to discriminate between open water bodies and other land cover. The SAR dataset consisted of C-band ENVISAT ASAR WSM images because of high frequent, large-area coverage, easy access and moderate spatial resolution.

A simple thresholding algorithm based on the temporal variability (TV) of the SAR backscatter and minimum backscatter (MiB) after normalization at 50^0 estimated from local incidence angle, slope, intercept of 22 images.

While this study focused on mapping permanent water bodies, the approach presented here is in theory applicable also to monitor the dynamic of water bodies by using spatio-temporal SAR data from selected time window. Assessing the detection of water surfaces in consequence of temporary events like inundation and flooding would require dense time series of measurements in correspondence of specific event. The upcoming of very high frequent observations of Sentinel-1 data could be used to demonstrate the capability of time series of short-term TV and MiB to track water dynamics in tundra regions.

7. Acknowledgements

The authors would like to thank Vienna University of Technology for support us the data and software to do this research.

References

[1] A. Bartsch, A. M. Trofaier, G. Hayman, D. Sabel, S. Schlaffer, D. B. Clark, and E. Blyth, "Detection of open water dynamics with ENVISAT ASAR in support of land surface modelling at high latitudes," Biogeosciences, vol. 9, no. 2, pp. 703–714, Feb. 2012.

[2] A. Bartsch, C. Pathe, W. Wagner, and K. Scipal, "Detection of permanent open water surfaces in central Siberia with ENVISAT ASAR wide swath data with special emphasis on the estimation of methane fluxes from tundra wetlands," Hydrol. Res., vol. 39, no. 2, p. 89, Mar. 2008.

[3] A. Bartsch, W. Wagner, K. Scipal, C. Pathe, D. Sabel, and P. Wolski, "Global monitoring of wetlands - the value of ENVISAT ASAR Global mode," J. Environ. Manage., vol. 90, no. 7, pp. 2226–2233, 2009.

[4] S. Quegan and J. J. Yu, "Filtering of multichannel SAR images," Geoscience and Remote Sensing, IEEE Transactions on, vol. 39, no. 11. pp. 2373–2379, 2001.

[5] C. Pathe, W. Wagner, D. Sabel, M. Doubkova, and J. B. Basara, "Using ENVISAT ASAR Global Mode Data for Surface Soil Moisture Retrieval Over Oklahoma, USA," IEEE Trans. Geosci. Remote Sens., vol. 47, no. 2, pp. 468–480, Feb. 2009.

[6] J. Reschke, A. Bartsch, S. Schlaffer, and D. Schepaschenko, "Capability of C-Band SAR for Operational Wetland Monitoring at High Latitudes," Remote Sens., vol. 4, no. 12, pp. 2923–2943, Oct. 2012.

[7] M. Silveira and S. Heleno, "Separation Between Water and Land in SAR Images Using Region-Based Level Sets," Geoscience and Remote Sensing Letters, IEEE, vol. 6, no. 3. pp. 471–475, 2009.

[8] M. Santoro and U. Wegmuller, "Multi-temporal Synthetic Aperture Radar Metrics Applied to Map Open Water Bodies," Selected Topics in Applied Earth Observations and Remote Sensing, IEEE Journal of, vol. PP, no. 99. pp. 1–14, 2013.

[9] A. Wendleder, B. Wessel, A. Roth, M. Breunig, K. Martin, and S. Wagenbrenner, "TanDEM-X Water Indication Mask: Generation and First Evaluation Results," Selected Topics in Applied Earth Observations and Remote Sensing, IEEE Journal of, vol. 6, no. 1. pp. 171–179, 2013.

[10] C. Kuenzer, H. Guo, J. Huth, P. Leinenkugel, X. Li, and S. Dech, "Flood mapping and flood dynamics of the mekong delta: ENVISAT-ASAR-WSM based time series analyses," Remote Sens., vol. 5, no. 2, pp. 687–715, 2013.

[11] M. P. Makynen, A. T. Manninen, M. H. Simila, J. A. Karvonen, and M. T. Hallikainen, "Incidence angle dependence of the statistical properties of C-band HH-polarization backscattering signatures of the Baltic Sea ice," Geoscience and Remote Sensing, IEEE Transactions on, vol. 40, no. 12. pp. 2593–2605, 2002.

[12] P.-L. Frison and E. Mougin, "Use of ERS-1 Wind Scatterometer Data over Land Surfaces," IEEE Trans. Geosci. Remote Sens., vol. 34, no. 2, pp. 550–560, 1996.

[13] J. a. Shufelt, "Performance evaluation and analysis of monocular building extraction from aerial imagery," IEEE Trans. Pattern Anal. Mach. Intell., vol. 21, no. 4, pp. 311-326, Apr. 1999.

[14] G. M. Foody, "Status of land cover classification accuracy assessment," Remote Sens. Environ., vol. 80, no. 1, pp. 185–201, Apr. 2002.

Nghiên cứu khả năng chiết tách nước bề mặt từ dữ liệu viễn thám Radar đa thời gian khu vực đồng bằng sông Cửu Long

Nguyễn Bá Duy, Trần Thị Hương Giang

Đại học Mỏ - Địa Chất Hà Nội

Tóm tắt: Viễn thám Radar với những ưu điểm nổi trội như khả năng chụp xuyên mây, không phụ thuộc vào điều kiện thời tiết và chu trình ngày đêm đã được sử dụng rộng rãi để chiết tách nước bề mặt cũng như được áp dụng trong việc theo dõi mức độ lũ lụt ở những nơi có mây che phủ thường xuyên. Năng lượng tán xạ từ bề mặt nước được ghi nhận tại bộ cảm Radar thông thường rất nhỏ, do bề mặt nước có đặc điểm phẳng như mặt gương, tín hiệu Radar tới tương tác với về mặt nước sẽ phản xạ hoàn toàn, do đó dẫn tới năng lượng trở lại bộ cảm Radar gần như bằng 0. Chính vì lí do này mà bề mặt nước bề mặt xuất hiện trên ảnh Radar thường có nền màu tối. Tuy nhiên, do ảnh hưởng của góc tới cục bộ và gió gây ra một độ nhám nhất định của bề mặt nước dẫn đến tín hiệu quay trở lại bộ cảm SAR cao bất thường , thậm trí giá trị tán xạ ngược từ mặt nước còn cao hơn so với tán xạ từ các đối tượng thực phủ khác. Mặt khác đối với khu vực đồng bằng sông Cửu Long là vùng có mùa mưa kéo dài (bắt đầu vào tháng 5 và kéo dài cho đến tháng 11 hàng năm), kết quả là hầu hết các khu vực canh tác nông nghiệp đều ngập trong nước và vì thế tại các khu vực này trên ảnh Radar có giá trị tán xạ thấp, bằng với giá trị của các đối tượng nước bề mặt. Đây là một thách thức khi thực hiện việc chiết tách nước bề mặt từ dữ liệu ảnh SAR. Bài báo nghiên cứu khả năng chiết tách nước bề mặt trên cơ sở xử lý dữ liệu viễn thám Radar đa thời gian. Dữ liệu viễn thám ENVISAT ASAR, kênh C, chụp vào mùa khô đã được lựa chọn và sử dụng trong bài báo nhằm làm giảm thiểu ảnh hướng của điều kiện khí tượng (gió). Ảnh hưởng của góc tới cục bộ được loại bỏ trên cơ sở sử dụng hệ số góc (độ dốc) β được xác định từ liệu đa thời gian. Giá trị tán xạ ngược được chuẩn hóa về về góc tới 50^o trên cơ sở giá trị tán xạ ngược ban đầu và góc tới cục bộ. Sau đó, từ dữ liệu đa thời gian sau khi chuẩn hóa được lấy cực trị (cực tiểu). Dựa trên cơ sở phân tích ba thông số được chiết tách từ dữ liệu đa thời gian, bao gồm hệ số góc (độ dốc) β , độ lệch chuẩn (STD), và giá trị tán xạ cực tiểu (MiB), cho thấy tán xạ cực tiểu khi kết hợp với độ lệch chuẩn cho phép chiết tách nước bề mặt với độ chính xác cao nhất bởi sử dụng thuật toán phân ngưỡng đơn giản.